

The Multi Aperture Imaging Array

V. Zarifis, R. M. Bell Jr., L. R. Benson, P. J. Cuneo, A. L. Duncan,
B. J. Herman, B. Holmes, R. D. Sigler, R. E. Stone, and D. M. Stubbs
*Lockheed Martin Advanced Technology Center, 3251 Hanover Street,
Palo Alto, CA 94304*

R.L. Kendrick

W.M. Keck Observatory, 65-1120 Mamalahoa Hwy., Kamuela, HI 96743

R. G. Paxman and J. H. Seldin

ERIM International, Inc., P.O. BOX 134008, Ann Arbor, MI 48113

Mats G. Löfdahl

*Royal Swedish Academy of Sciences, Stockholm Observatory, SE-133 36
Saltsjöbaden, Sweden*

Abstract. A nine telescope imaging phased array is being demonstrated at the Lockheed Martin Advanced Technology Center in Palo Alto. The sparse array consists of nine afocal telescopes arranged in a Y-formation that are combined to a common focus in a Fizeau interferometer configuration. We have demonstrated diffraction limited performance over a 150 microradian field of view with broad band (500 to 800 nm) illumination. We have also used white light phase diversity wavefront sensing techniques to adjust the phasing of each separate telescope in a closed loop control, using point sources and extended imagery.

1. Introduction

The resolution of an imaging system depends on the size of the collecting aperture and as such it is becoming more difficult to increase that without using huge monolithic optics. One approach is to use segmented optics which require precise alignment and phasing to reach the diffraction limit. Another revolutionary approach is to use multiple separate telescopes phased together, much as the field of radio astronomy has done many years ago. This concept of creating a high resolution, large aperture telescope by combining several smaller telescopes was first discussed by Michelson with reference to a stellar interferometer in 1920 (Michelson & Pease 1921). The initial concept was developed for determining the diameter of stars and as such is limited to a field of view on the order of nanoradians. Extending the field of view is a much more rigorous demonstration in which several design issues must be considered. The utility of this concept extends from ground based astronomical telescopes (Beckers 1991)

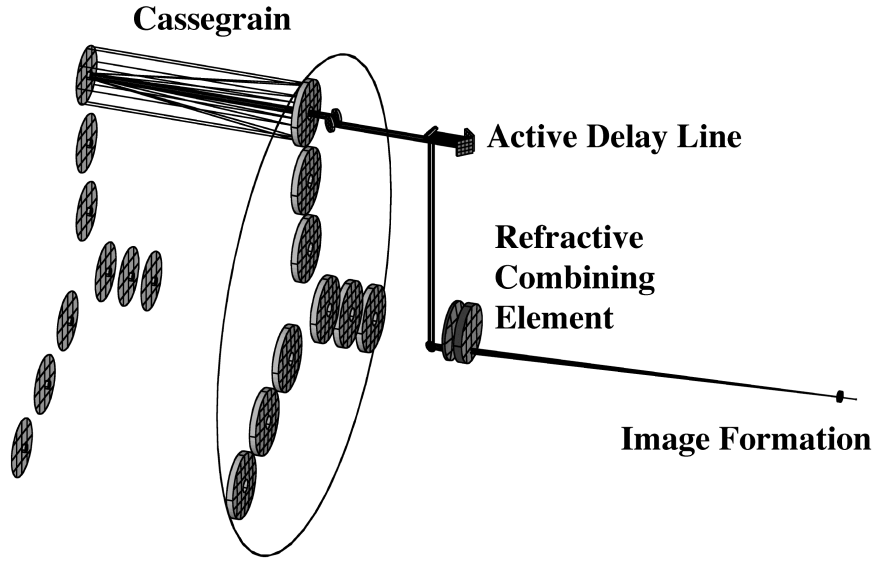


Figure 1. Optical layout of the imaging array.

to space based observatories and planetary exploration missions. In this paper, we discuss what we believe are the first results of a broad band multiple telescope imaging array phased over a significant field of view. It is also a validation that phase diversity techniques can keep the individual telescopes phased in a closed-loop control with broadband light and extended imagery (Kendrick et al. 1994). This work builds on previous demonstrations of phased arrays (Hege et al. 1985; Fender & Carreras 1988; Dehainaut et al. 1988) that have proven the concept of phasing separate telescopes but were limited to either very narrow spectral band or a field of view that was nearly zero.

2. The Multi Aperture Array

In order to get diffraction limited performance from a multiple telescope imaging array over a significant field of view with a wide spectral band there can be no non-common refractive elements present in the optical path. Each of the telescopes described here is entirely reflective, thereby avoiding this problem. In addition, the magnification of each telescope of the array must be matched to a level that results in minimal aberrations as a function of field angle. This is achieved by carefully matching the individual telescope mirror radii of curvature with resulting magnification differences to less than a 1%. There are other important design considerations such as polarization maintenance in all the beam

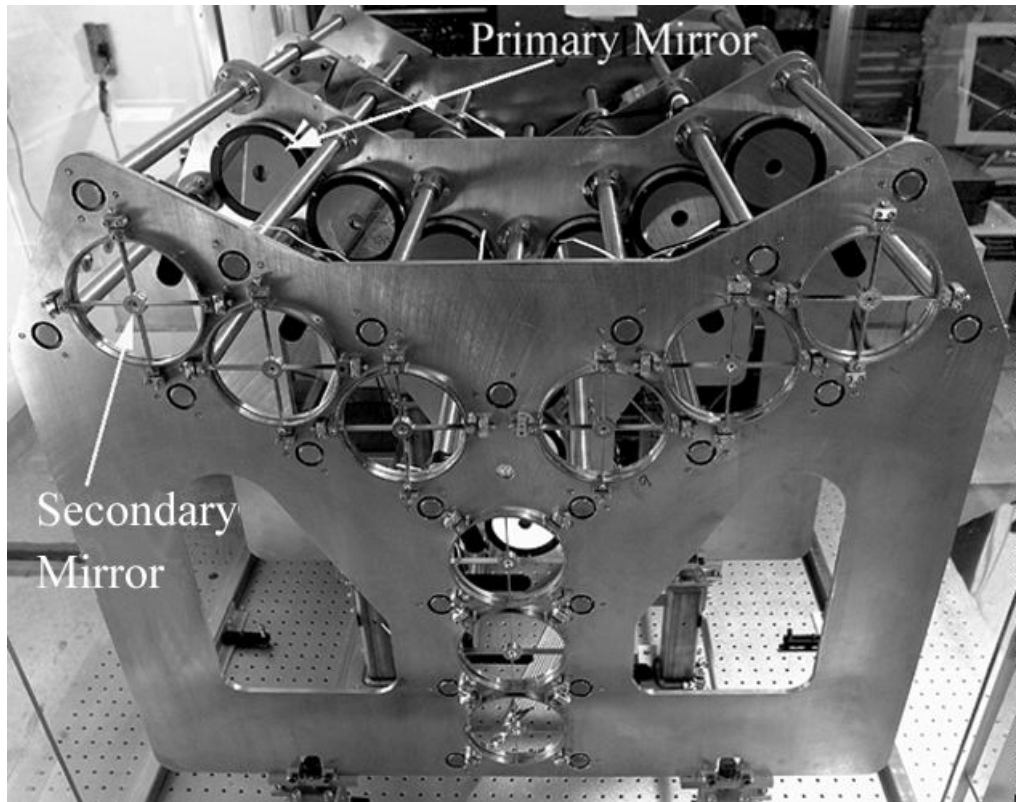


Figure 2. Front view of the imaging array.

paths and exact pupil geometry matching. These were carefully addressed in our design so as to achieve a diffraction limited field of view of 150 microradians, limited only by vignetting at the beam combiner.

Figure 1 is a diagram of the optical layout of the phased array. Rays are traced for one of the telescopes. Each telescope is an afocal Dahl-Kirkham Cassegrain with a 10 cm clear aperture. The telescopes have a magnification of 10 so that the outgoing beam is 1 cm in diameter. Following the telescope is a set of fold flats that are used to adjust the telescope pointing and pupil geometry. Beyond those, the rays fall on a front surface roof prism that is mounted to a piezoelectrically actuated stage. This active delay line controls the optical path-length of each telescope. The stage has a total range of 25 mm and a step resolution of approximately 4 nm. The beam is then directed into the refractive combining element with two fold flats. This design allows for adjustment of all 6 degrees of freedom in each telescope. All the beams are relayed in front of the combiner in the exact configuration of the entrance pupil. Each individual telescope has an effective $f/\#$ of 165. The longest baseline in the nine aperture array is 0.65 m giving an effective $f/\#$ of 21 for all nine telescopes. The diffraction-limited field of view for the entire array is approximately 150 microradians. We are using a liquid cooled Photometrics PXL camera with an EK KAF-1400 CCD detector. The detector array has a 100% fill factor with 6.8 micron square pixels

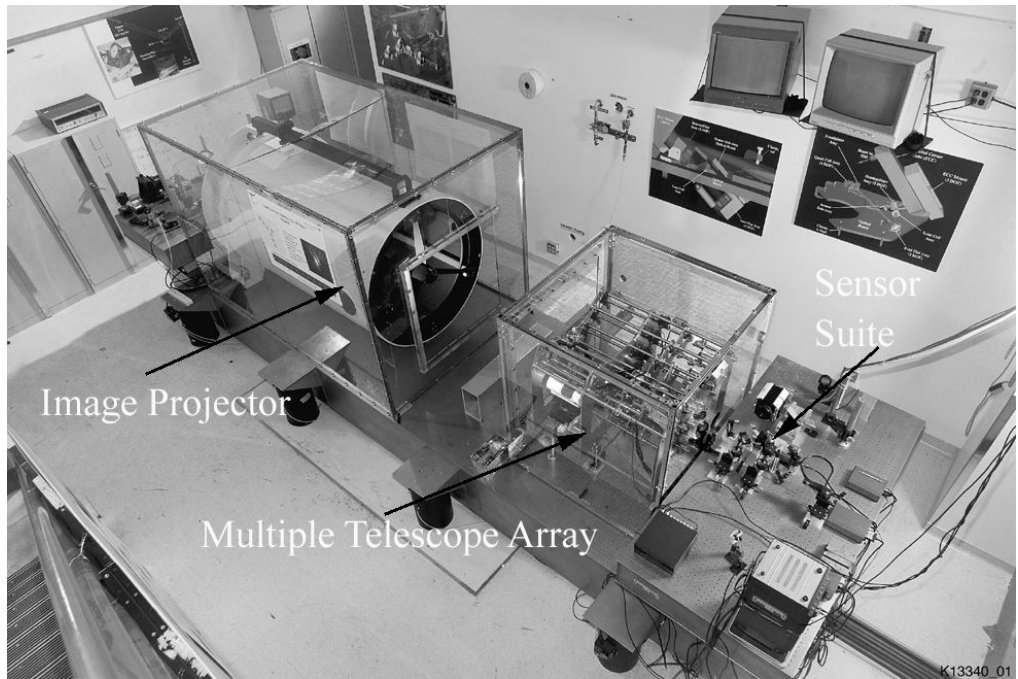


Figure 3. Test Bed in Palo Alto. The long side of the optical table is 20 ft.

and a full well capacity of 42k electrons. The read-noise is 10 electrons rms when cooled to $-25\text{ }^{\circ}\text{C}$. The 6.8 micron pixel size critically samples the image for the nine telescope array at a wavelength of 0.62 microns. The camera analog data output is digitized to 12 bits and processed on a SUN workstation. The piston and tilt adjustments for each telescope are also controlled from a similar workstation.

Figure 2 is a front view of the array. The array support structure is fabricated completely of Invar for thermal and mechanical stability. The structure consists of 3 major flat plates held rigidly by twenty one 19 mm diameter solid Invar rods. The rods maintain the critical spacing between each of the optical elements. The plates and rods can be seen clearly in Figure 2 as can the individual telescope primary mirrors and secondary spider supports. In order to facilitate the alignment process, the structure was precisely assembled holding position tolerances to within 0.1 mm.

Figure 3 shows the positioning of the fully assembled array on the imaging test bed in Palo Alto, CA. A 0.8 m diameter collimating telescope is used to project images into the array. Point source and extended targets are placed at the focus of the projection telescope and illuminated with broadband sources. Point source data is used to initially align and phase the telescopes.

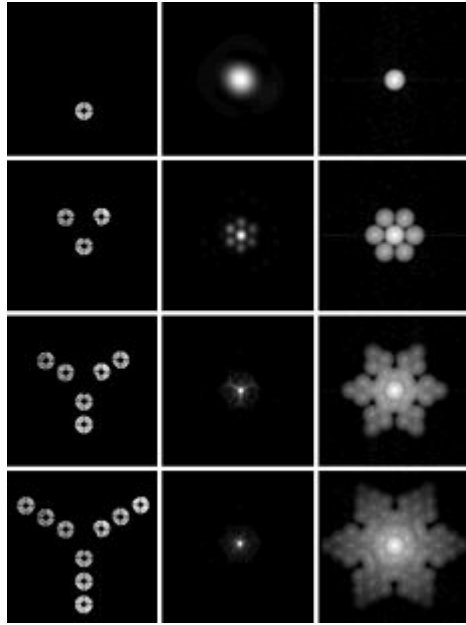


Figure 4. Point source images with different aperture configurations. The left column shows the pupil configurations, the middle shows the PSF, and the right is the log-enhanced image of the MTF for each configuration

3. Results

Figure 4 shows point source data for 1, 3, 6, and 9 apertures of the array. The aperture configuration is shown along with the Point Spread Function (PSF) and the Modulation Transfer Function (MTF). The MTF is calculated by taking the modulus of the inverse Fourier transform of the PSF and shown in a log intensity scale to enhance the details.

The data in Figure 4 was acquired with a bandwidth of 50 nm centered around 625 nm. The narrow bandwidth was used to accentuate the features of the MTF and PSF. The MTF plots show clearly that the array performed at the theoretical resolution for a zero field of view. An extended scene was used to verify the performance over the 150 microradian field. The images in Figure 5 are of a standard bar target illuminated with broadband (500-800 nm) light.

The focal plane images need to be reconstructed to account for the effects of the phased array imaging system. Each of the images has been reconstructed with a standard maximum entropy algorithm using point-source images as the PSF's. These images were recorded at the beginning and at the end of the image collection. One aperture cannot resolve any of the bars in the bar groupings that are displayed. Six phased apertures can resolve the 3:6 grouping which is nearly the diffraction limit for this Y-configuration of six apertures. (Group 3:6 is the sixth row of bars in the column under the number 3 (upper right corner) and corresponds to 1.3 microradians at 0.62 microns.) Some early data for the nine aperture configuration shows the expected resolution enhancement close to the

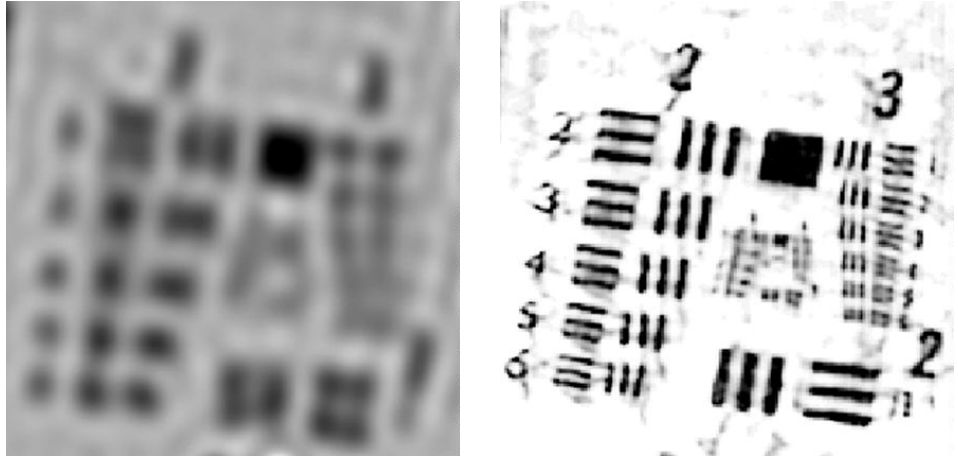


Figure 5. Reconstructed images from one (left) and six apertures (right). Six apertures resolve to the 3:6 grouping close to the expected diffraction limit.

4:3 grouping near the center of the target. The maximum resolution with the nine apertures is then 0.92 microradians at 0.62 microns. However, our scene projector has some residual aberrations near the field edges which affect the nine aperture imaging. These aberrations, along with the decreased fill ratio, make the resulting images appear less than optimal. Oversampling in the focal plane would increase the detector MTF allowing these areas to be better resolved.

4. Closed-loop control

Phase diversity techniques have been proposed for identifying and correcting wavefront distortions (Paxman & Fienup 1988) and have been used successfully to demonstrate the phasing of a segmented flat mirror (Kendrick et al. 1994). We have employed a broadband-illumination, model-based phase diversity algorithm, discussed elsewhere (Seldin et al. preprint), to keep the array phased in a closed-loop control setup. Our phase diversity sensor uses a simple optical design that produces two images of the object, one in focus and the other slightly defocused. The wavefront distortion is estimated from the intensity maps of these images. Phase corrections are derived using a maximum likelihood algorithm and applied in a closed-loop fashion to the optical delay lines of each telescope. The data is shown in Figure 6, where an impulse disturbance of 0.33 waves of piston is applied at the same time to two of the six phased apertures. The closed-loop control brings the system back in phase within a few quick iterations. The advantage of this method is that it does not require any reference beams for wavefront sensing and it can be used independently of the scene content. Ongoing research efforts are exploring other phase diversity algorithms and training-set-data based neural net algorithms to scale up the controlled number of apertures.

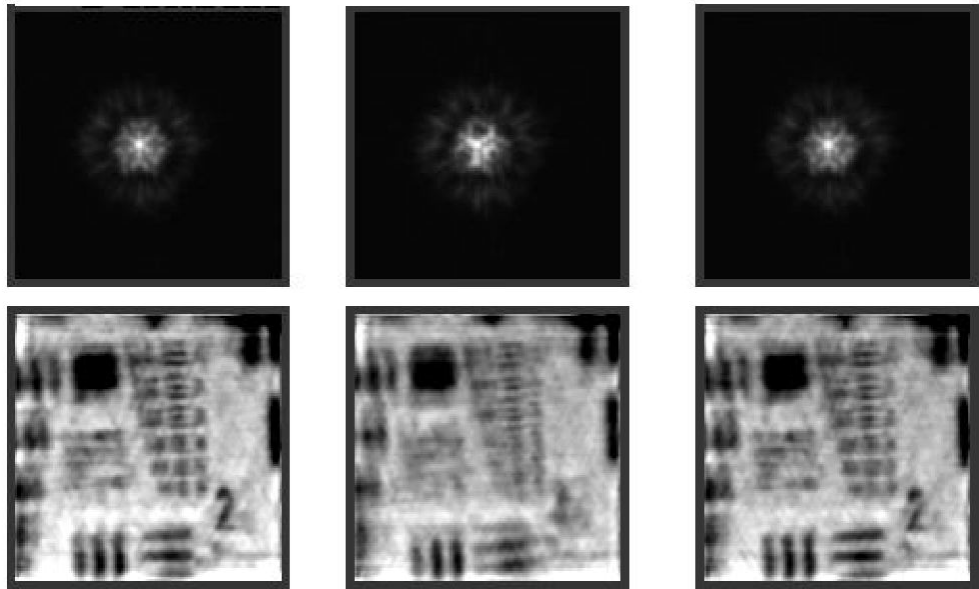


Figure 6. Closed loop data for disturbances on two apertures independent of the scene content. Left – initial phased images for point source (upper) and extended scene (lower). Middle – effect of impulse disturbance. Right – the recovered images.

5. Conclusions

We believe that the multiple phased telescopes is the one of the more elegant solution for future high resolution imaging systems. The data presented here demonstrates this concept in the laboratory environment. It is also shown that the phase diversity technique can be used as a simple wavefront sensor that can be applied to this type of phasing problem. Despite the fact that most of the discussion here focused on sparse aperture systems, the same approach can be applied to filled aperture systems. This results in relaxing some of the more stressing tolerances which exist in a single segmented-aperture phased telescope.

References

- Beckers, J. M. 1991, *J. Optics (Paris)*, 22, 73
 Dehainaut C. R., Hentz K. P., Weaver L. D., & Gonglewski J. D. 1988, *Opt. Eng.*, 27, 736
 Fender J.S. & Carreras R. A. 1988, *Opt. Eng.*, 27, 706
 Hege, E. K., Beckers J. M., Strittmatter P. A., & McCarthy D. W., 1985, *Applied Optics*, 24, 2565
 Kendrick, R. L., Acton, D. S., Duncan, A. L. 1994, *Appl. Opt.*, 33, 6533
 Michelson A. A. & Pease F. G. 1921, *ApJ*, 53 249

Paxman, R. G. & Fienup, J. R. 1988, J. Opt. Soc. Am. A, 5, 914
Seldin, J. H., et al. preprint